FIFI LS: the optical design and diffraction analysis

W. Raab, L. W. Looney, A. Poglitsch, N. Geis, R. Hoenle, D. Rosenthal, R. Genzel

Max-Planck-Institut für Extraterrestrische Physik (MPE), Postfach 1312,
D-85741 Garching, Germany

ABSTRACT

We present the optical system of the Field-Imaging Far-Infrared Line Spectrometer (FIFI LS) for the SOFIA airborne observatory. The instrument is designed to allow diffraction limited integral field spectroscopy in the far infrared wavelength range 42 to 210 microns. Two parallel wavelength channels (42 - 110 microns and 110 - 210 microns) employ Littrow mounted diffraction gratings with anamorphic collimators. Mirror image slicers in each channel rearrange the 5 x 5 pixel field of view along the 1 x 25 entrance slit of the grating spectrograph. The spectral resolution varies in the range of R = 1400 - 6500, depending on observing wavelength. The optical components in the image slicer is comprised of several mirrors with physical dimensions on the order of a few tens of wavelength. Consequently diffraction effects are a serious concern in the design of the optical system. Substantial effort in modeling diffraction effects throughout the optical system and its impact upon the expected performance of the instrument have been made. The results of the scalar diffraction analysis carried out with a commercial software package has been confirmed by a full vectorial analysis, showing negligible dependence of the diffraction effects on the polarization properties of the electromagnetic field.

Keywords: Integral Field Imaging, Spectrometer, Far-Infrared, image slicer, FIR, FIFI LS, FIFI, SOFIA, diffraction

1. INTRODUCTION

To investigate the morphology and dynamics of extended structures astronomers rely heavily upon so called 3-dimensional imaging, where both spectral (radial velocity) and spatial (the two dimensions of the image field) information are obtained simultaneously. Practically every type of spectrometer suffers difficulties in imaging the three astrophysical dimensions onto a two dimensional detector array. Classical types of spectrometers force the observer to preferentially choose two of the three dimensional quantities: for a long slit spectrometer a range of one spatial and one spectral coordinates at a given spatial coordinate and for a Fabry-Perot spectrometer a range of two spatial coordinates at a given wavelength coordinate.

Nonetheless, long slit spectrometers as well as Fabry-Perot spectrometers are frequently used in astronomical instruments, because of their comparatively easy design. To access the respective missing dimension, the observer using one of these spectrometers has then to spatially scan the single long-slit spectrometer across the extended source, or spectrally scan a Fabry-Perot spectrometer across the wavelength coordinates of interests. In addition to a dramatic decrease of observing efficiency, the scanning technique adds another a layer of difficulty: in the time taken to change the pointing or scan the Fabry-Perot, the observing conditions (e.g. seeing or pointing errors) or instrumental responsivity may drift, adding systematic noise to the data cube.

In this paper we present the optical design of the the Far-Infrared Field-Imaging Line Spectrometer (FIFI LS) instrument,[1] utilizing an image slicer technique for the first time in the far-infrared. Besides its obvious strength of obtaining a complete datacube in one single observation, the 3D imaging technique also produces highly reliable datasets due to the parallel and simultaneous data acquisition.

Scaling image slicing techniques successfully demonstrated in the near infrared,[2] which utilize flat mirror systems is not without problems: conservation of energy dictates that the product of collecting area and accepted solid angle of the optics is directly proportional to the square of the wavelength, making flat mirror image slicers prohibitively large for long wavelength applications. A large concern in the design of a far-infrared image slicing system is unavoidable diffraction effects, since some of the employed mirrors are not larger than a few tens of the observing wavelength. Utmost care in analyzing the consequences of diffraction effects must therefore been taken to avoid any degradation of the instrument capabilities.

email: raab@mpe.mpg.de; http://fifi-ls.mpe-garching.mpg.de

Airborne Telescope Systems II, Ramsey K. Melugin, Hans-Peter Röser, Editors,
Proceedings of SPIE Vol. 4857 (2003) © 2003 SPIE · 0277-786X/03/$15.00

2. OPTICAL DESIGN

2.1. Basic Properties

FIFI LS (see also[3]) is a two channel spectrometer which allows simultaneous observations in the wavelength bands 42 - 110 μm and 110 - 210 μm. The key to the 3D imaging capability is an image slicer system in each band, that rearranges the two dimensional 5×5 pixel field along a 25 (+4)×1 pseudo-slit (Fig.1) which can be easily fed into a grating spectrometer. Notice the deliberate 1 pixel gap between the 5 individual slices eliminating cross-talk between spatial pixels that are not adjacent in the 2-dimensional field of view like pixel I and II in Fig.1. In each channel, a large format 25×16 pixel detector array is utilized.[4,5]

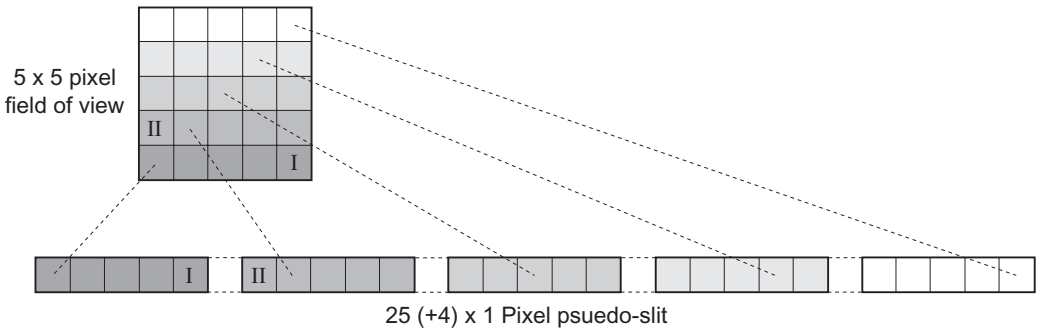

Figure 1. A detail showing the basic design premise for the FIFI LS image slicer. The optics must slice the rows of the 5×5 pixel field of view into a 25×1 pixel pseudo-slit. The gaps in the slit are added to reduce cross-talk between nonadjacent field pixels (e.g. pixels I and II).

2.2. Optical Layout

In Fig.2 we present a schematic overview of the FIFI LS optical layout in block format. The first optical component in the optical path is an adjustable dichroic beam splitter which reflects incoming infrared radiation into the FIFI LS cryostat and passes the visible and near-infrared radiation to a CCD guider camera. The reflected beam enters the vacuum vessel via a thin polypropylene window. The following entrance optics is cooled to 77 K in order to minimize background radiation. The entrance optics consists of a K-mirror assembly that is situated close to the focus of the SOFIA telescope used to compensate for sky rotation during integration and an elliptical Re-imaging mirror, which refocuses the diverging beam onto the Slicer mirrors. The Re-imaging mirror also creates a pupil right where the beam enters the actual spectrometer part of the instrument which is cooled to 4 K, forming a Lyot-Stop to minimize straylight. A second dichroic beam splitter close to the Lyot-Stop reflects long wavelength radiation (110 - 210 μm) and transmits short wavelength radiation (42 -110 μm) thus separating the Blue and Red band of the instrument. The blue and red channels of the spectrometers are designed similar, but are not exact copies of each other: the Blue channel has pixels that are a factor of 2 smaller on the sky, the beam is magnified by a system of three elliptical mirrors before entering the slicer assembly.

As shown schematically in Fig.1, the major driving design goal of the image slicer assembly is to optically rearrange the two dimensional field of view into a one dimensional pseudo-slit that can be fed into a standard long slit spectrometer. In FIFI LS the slicer system is comprised of three sets of mirrors in groups of 5 (Fig.3). The first stack of 5 mirrors (Slicer mirrors; R2a-R2e) are slightly tilted with respect to the center slice, and spatially fan-out each row of the two dimensional field of view. The Slicer mirrors have spherical surfaces that image the pupil onto the second set of mirrors (Capture mirrors; R3a-R3e) in the slicer system. In the next step, the Capture mirrors, designed as on-axis spherical biconics, refocus the beam onto the last mirror in the set of 3 slicer system mirrors (Slit mirrors; R4a-R4e), forming the one dimensional pseudo-slit. The Slit mirrors again are spherical mirrors that are angled such that the 5 pupils are virtually re-imaged to a single pupil, which is then imaged onto the diffraction gratings by two anamorphic collimators. Since the gratings are mounted in Littrow configuration, the same collimators are can be used to refocus the dispersed beam at the output. In an ideal Littrow mounted system, the input and output beams

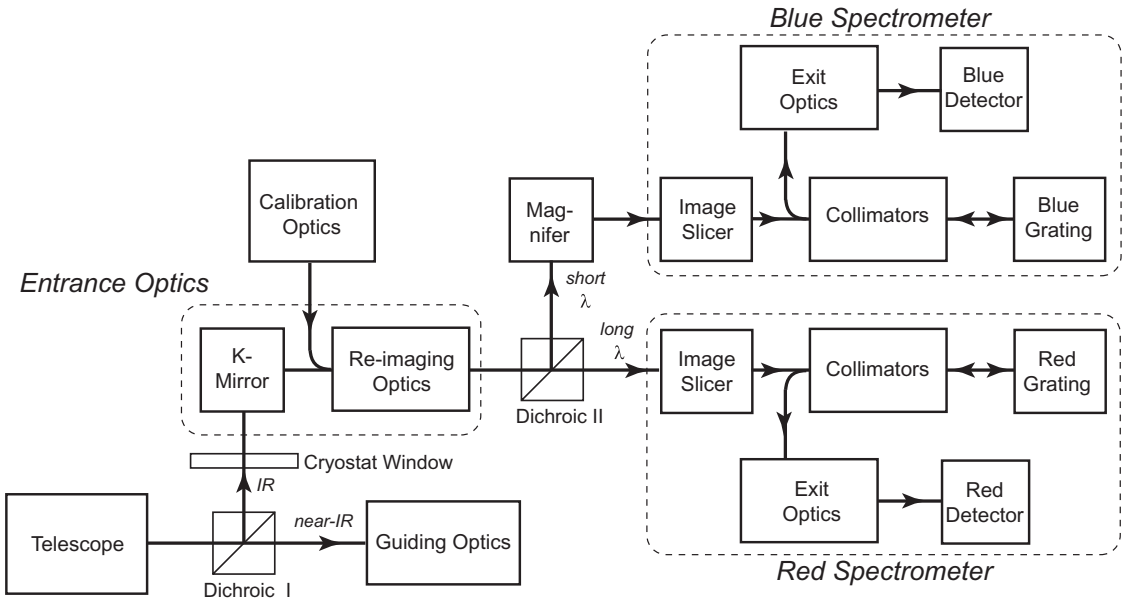

Figure 2. A simplified schematic overview of the FIFI LS optics. Calibration optics and intensity sources can be switched into the path via a flip-mirror to provide flat-fielding of the detector pixels.

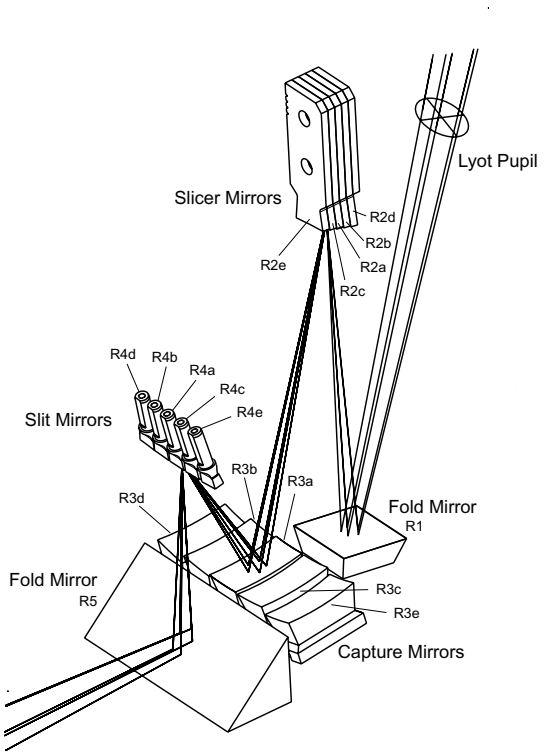

Figure 3. Close up view of the slicer mirror components for the Red channel with only the rays of the central slice shown. The Blue channel is similar.

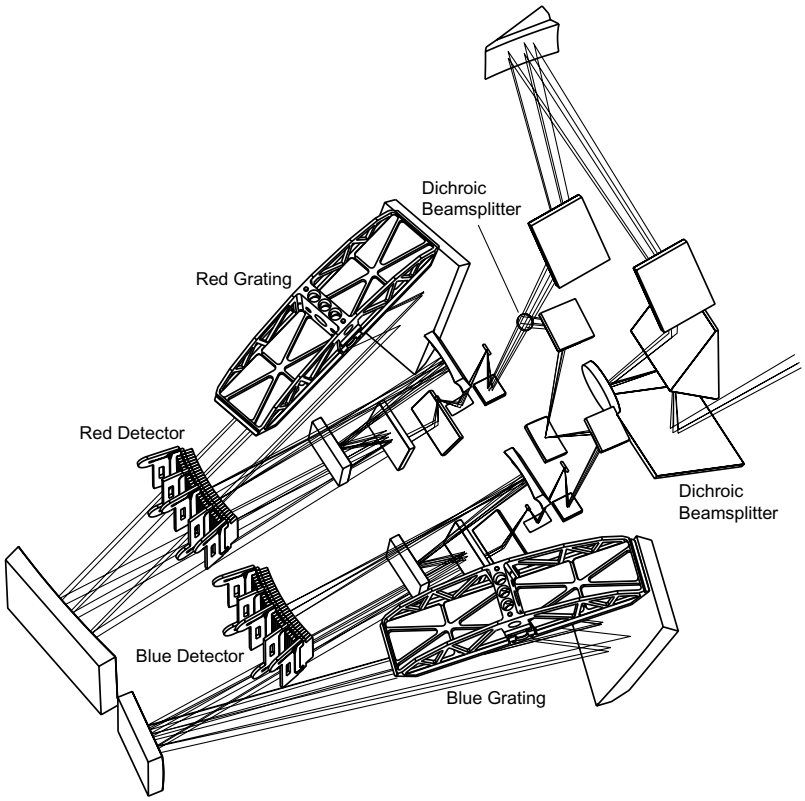

Figure 4. The FIFI LS optical system.

coincide, which is impractical for a real system, so the optics are designed with a 1.8° divergence between incoming and outgoing beam.

After spectral multiplexing in the spectrometers, anamorphic exit optics are used to scale the spectrum to accommodate the detector array dimensions in the spectral as well as in the spatial direction. The exit optics also form a pupil at a distance of 240 mm in front of the detector. Together with light cones attached in front of the individual pixel that are designed to accept light from only a solid angle defined by this pupil. This arrangement forms a highly efficient straylight suppression system. Fig.4 shows a 3D-representation of the overall optical layout. The Red channel is located in the upper, the Blue channel in the lower part of the image.

3. OPTICAL PERFORMANCE

3.1. Ray Trace Analysis

The optical design of the entire FIFI LS optics has been performed using the software package Zeemax V.10. Some selected results of this ray trace analysis are presented in this section. As mentioned before, the FIFI LS image slicer creates the pseudo-slit focus on the Slit mirrors. As shown in Fig.5, there is significant curvature of the pseudo-slit in the red channel as well as in the blue channel. This effect arises from the geometric design of the individual components which reflect radiation out of the incoming beam plane, optically corresponding to a rotation around the optical axis and a smile/frown of the pseudo-slit. Since the diffraction gratings are also tilted with respect to the main beam, they also display an output wavelength dependent slit curvature. The image slicers are designed in a way to counteract and completely cancel the expected grating slit curvature at approximately 60 μm and 160 μm. Fig.6 shows how this design successfully eliminates any slit curvature on the Red detector at a wavelength of 160 μm. However, in the Blue channel (not shown here), the grating curvature is less pronounced so less curvature in the pseudo-slits is required.

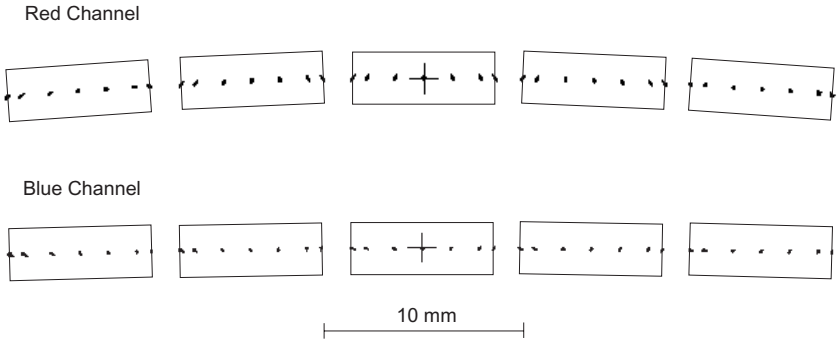

Figure 5. Simulation of the SOFIA telescope re-imaged focus on the Slit mirrors. This is exactly equivalent to the entry slit of a long-slit spectrometer.

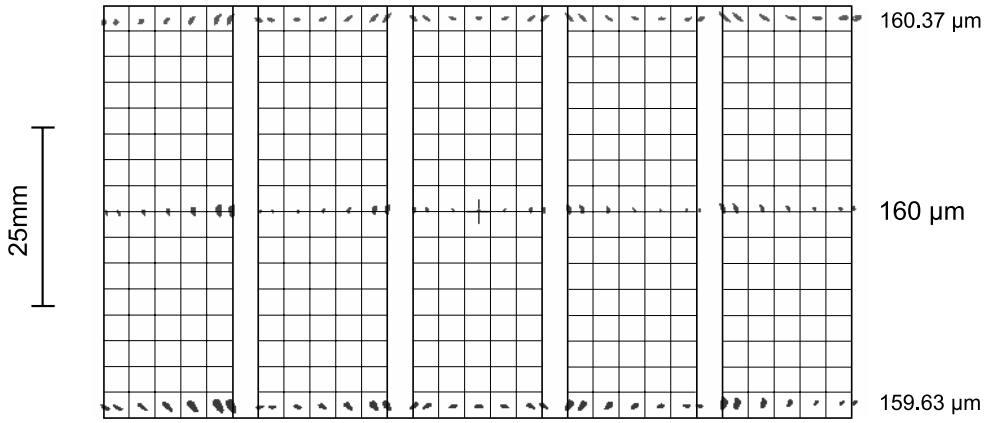

Figure 6. The final imaging of the dispersed beam at a wavelength of 160 μm in the long wavelength channel.

3.2. Diffraction Analysis

Diffraction limited performance, one of the most important requirement of FIFI LS, as well as geometrical light loss effects due to cutting into the diffraction pattern calls for oversizing of the optical components in order to prevent any significant deterioration of the instrument resolution or sensitivity on the one hand. On the other hand, practical constraints such as geometry, limited instrument size, and straylight concerns usually do not allow indefinite enlargement of the individual mirrors. To find the optimal mirror sizes and to calculate the spectral resolution and light loss throughout in the instrument, detailed modeling of diffraction effects have been performed using the software package GLAD Version 4.5. In addition, a full vectorial analysis has been carried out to check for polarization dependent diffraction effects. Detailed analysis was performed of both the Red and Blue channels, but as they are very similar, only the Red channel diffraction effects are discussed in the following subsections.

3.2.1. Scalar Analysis

Due to their size of only 3 × 15 mm corresponding to 20 wavelengths at 150 μm, the Slicer mirrors are cutting significantly into the Airy disk of the telescope, causing strong diffraction from that point on. For this analysis, all optics in front of the slicer system, including telescope, are assumed to be adequately oversized that no diffraction losses are seen before the slicer mirrors.

Fig.7 shows the calculated diffraction pattern on the respective mirrors of the slicer system. Notice the significant cutting of the Slicer mirror into the diffraction pattern of the telescope illustrated in the upper half of Fig.7. As a direct consequence, the diffraction pattern on the Capture mirrors shows strong sidelobes in the direction perpendicular to the long side of the Slicer mirrors. The size of the Capture mirrors has been chosen to conserve the first sidelobes of

the intensity distribution. The calculated pattern on the Slit mirrors shows how the slicer system has been successfully designed such that almost all flux impinging on the Slicer mirrors is refocused without significant widening of the diffraction pattern.

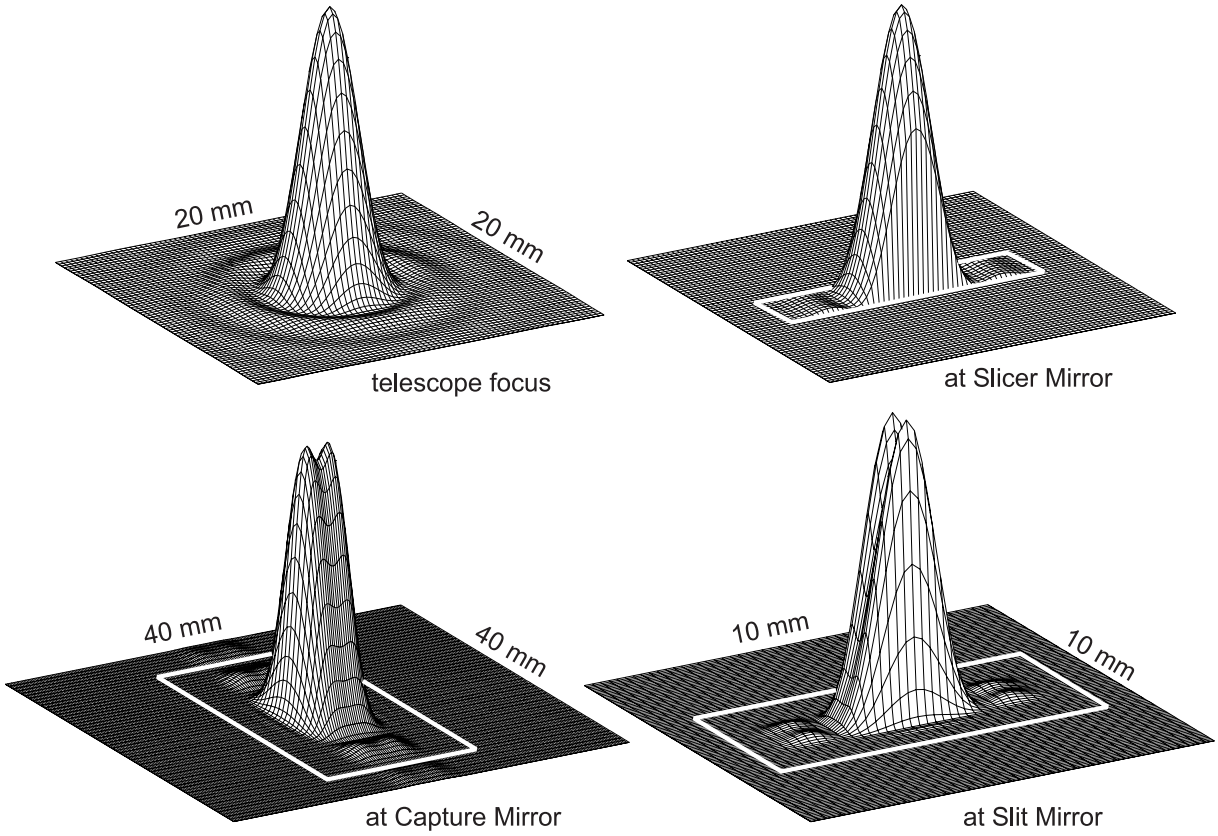

Figure 7. The diffraction effects of the three slicer mirrors of the central slice as estimated by using a scalar solution.

The diffraction pattern on the gratings is of special interest, because it defines the illumination as well as the spectral resolution of the diffraction gratings. Fig.8 illustrates the intensity distribution on the grating at the extreme wavelengths of 110 μm and 210 μm, together with the band center wavelength of 160 μm. The figure shows how the illumination and therefore also the spectral resolution of the grating increases with increasing wavelength until the grating is overilluminated at a wavelength around 180 μm. Finally Fig.8 also shows the effect of all the combined diffraction analysis at the detector pixel. The pixel size is well sampling the diffraction pattern on the detector.

3.2.2. Full Vectorial Analysis

The scalar analysis diffraction analysis has an obvious deficiency: a real electromagnetic field can not be accurately described as a simple scalar field. For the correct treatment of an electromagnetic wave a complete set of 3-dimensional vector functions describing the local component of the electric and magnetic field vectors is necessary. Accordingly, important effects that might play a major role, such as polarization dependent diffraction can not be investigated by a simple scalar analysis. To probe the differences between the scalar analysis and a numerical solution of the vector equations,[6,7] the diffraction pattern on the Slicer and Capture mirrors have been compared (see also[8]). Fig.9 illustrates the results of the vectorial analysis. The scalar as well as the vectorial analysis are qualitatively in perfect agreement, showing that polarization dependent diffraction effects are negligible. Thus, the simpler scalar approximation well describes the effects of the FIFI LS optics.

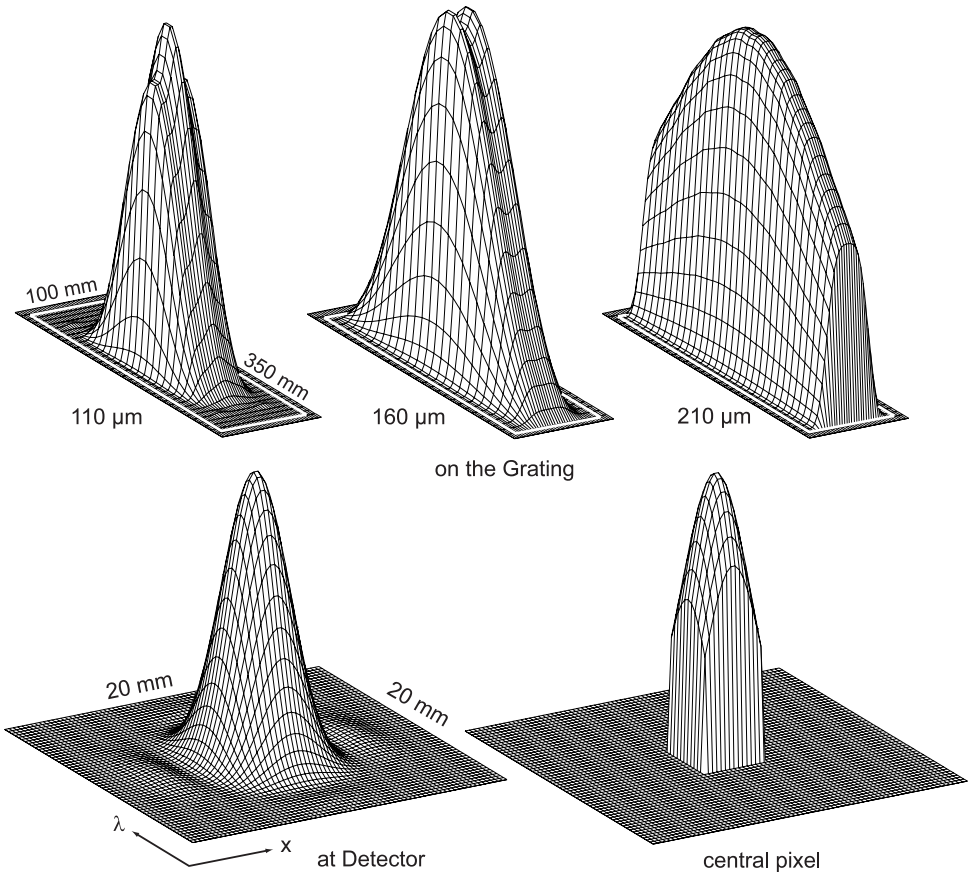

Figure 8. The diffraction effects in the Red channel that arise mainly from the slicer system on the grating at three wavelengths and on the central pixel of the detector at 160 μm.

3.3. Throughput

One important results of the diffraction analysis is an estimation of the light loss on the individual optical components and its relative effect on the overall throughput of the spectrometer. Fig.10 illustrates the integrated light loss from diffraction after each mirror surface, normalized to 100% light at the Slicer mirrors. As the analysis shows, most of the light is lost after the capture mirrors of the slicer assembly, which by design cuts into the diffraction pattern of the Slicer mirrors. Another significant source of light loss is the first Collimator mirror, which could not designed any larger due to limited space in the instrument. Nonetheless, the light loss caused by diffraction and vignetting are minimal (<6% at most operating wavelengths) compared to the two largest contributions of the overall FIFI LS throughput, which are the quantum efficency of the detectors (∼30%) and the gratings efficiency (median efficency ∼70%).

3.4. Spectral Resolution

As mentioned before, diffraction effects directly affect the illumination of the diffraction gratings and consequently determine the spectral resolution of the instrument. We calculated the diffraction as an effective aperture of the grating at various tilts, defined by the observing wavelength. As in the real system, the effect of pixel sampling is taken into account by convolving the spectral response function with a 3.6 × 3.6 mm square corresponding to the spatial dimensions of a detector pixel. Fig.11 shows the spectral resolving power, defined as the FWHM of the spectral response line as a function of the observing wavelength together with the spectral response line at 160 μm to illustrate the slight decrease of the spectral resolution due to the discrete pixel sampling.

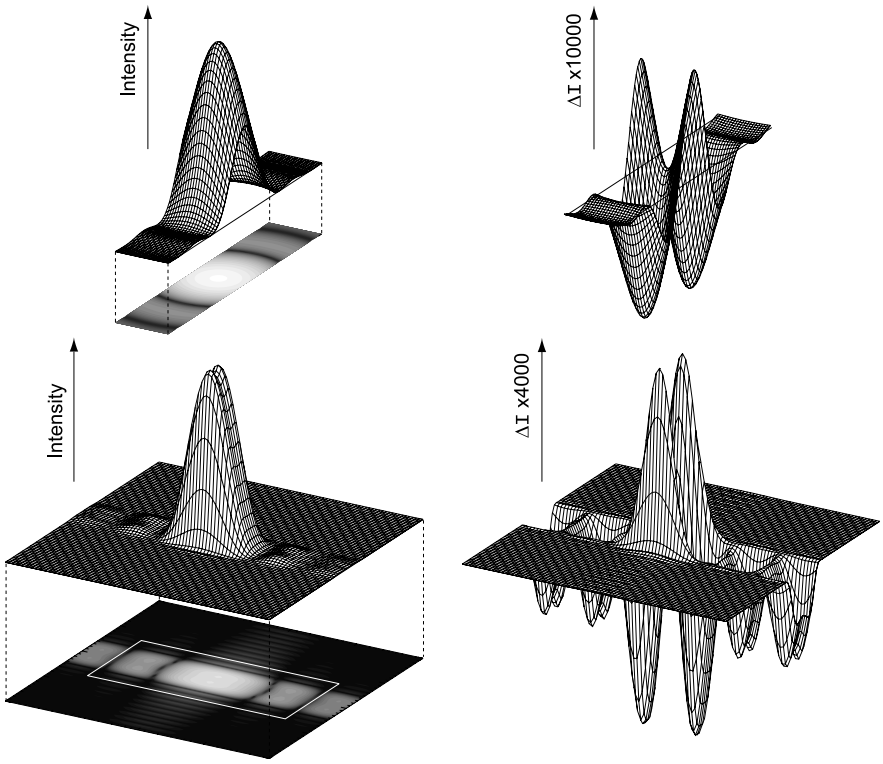

Figure 9. The diffraction effects on the slicer and capture mirrors calculated using the vectorial treatment on the left. On the right, the differences between two polarizations. The polarization difference on the top is most likely numerical rounding errors, and those on the bottom are real variations but insignificant.

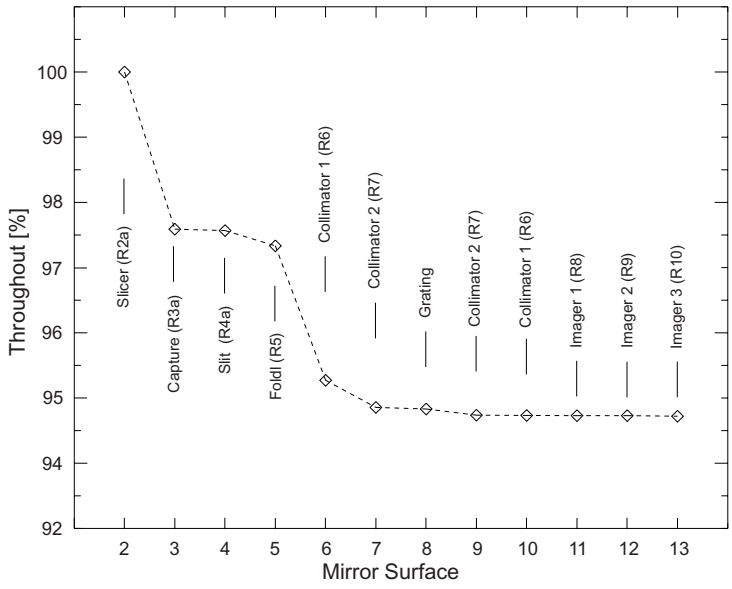

Figure 10. The light loss thru the optics due to pure diffraction and vignetting effects. Note that the largest losses are from the slicer system and the first Collimator mirrors.

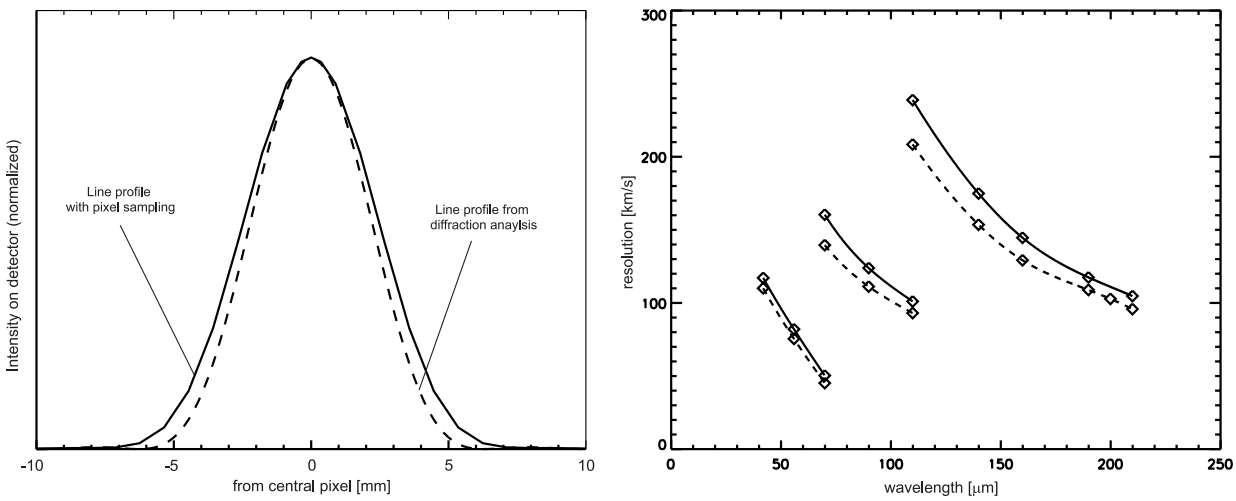

Figure 11. The simulated resolution of FIFI LS, including pixel sampling effects.

4. CONCLUSIONS

As has been shown in other wavelength bands, integral field instrumentation is a very useful tool to probe many astronomical problems. However until recently, far-infrared integral field instruments were not technically feasible due to the limited size of the detector arrays. With the construction of large format detectors, we have been able to design the first integral field instrument in the far-infrared using a novel design with reflective slicer mirrors. In this paper we presented the optical assembly of FIFI LS and showed by ray tracing as well as careful analysis of diffraction effects, how a reflective mirror slicer system can successfully be implemented in a far-infrared imaging spectrometer. Making use of the high spatial resolution and sensitivity on SOFIA, FIFI LS will provide a major step forward for far-infrared spectroscopy.

REFERENCES

1. L.W. Looney, W. Raab, A. Poglitsch, N. Geis, (2002) in preparation
2. A. Krabbe, L. Weitzel, H. Kroker, L. E. Tacconi-Garman, M. Cameron, N. Thatte, G. Samann, T. Boeker, R. Genzel, & . Drapatz, Proc. SPIE 2475, Infrared Detectors and Instrumentation for Astronomy, A. M. Fowler, ed., p. 172, (1995).
3. L.W. Looney, W. Raab, A. Poglitsch, N. Geis, D. Rosenthal, R. Hoenle, R. Klein, F. Fumi, R. Genzel, SPIE Proc, This volume (2002)
4. D. Rosenthal, J.W. Beeman, N. Geis, L.W. Looney, A. Poglitsch, W.K. Park, W. Raab, & A. Urban, SPIE Proc, 4014, p. 156 (2000)
5. R. Hönle, et al. (2004) in preparation
6. W.R. Smythe, Phys. Rev., 72, p. 1066 (1947)
7. J.D. Jackson, Classical Electrodynamics, second edition, *John Wiley & Sons*, pp. 432-438
8. W. Raab, Ph.D. Thesis, Ludwig-Maximilian University (2002)